65-fs Yb:CaF_2 laser mode-locked by SESAM

FEDERICO PIRZIO[1,*], SAMUELE D. DI DIO CAFISO[1,2], MATTHIAS KEMNITZER[2], FLORIAN KIENLE[2], ANNALISA GUANDALINI[2], JUERG AUS DER AU[2], AND ANTONIO AGNESI[1]

[1] *Dipartimento di Ingegneria Industriale e dell'Informazione, Via Ferrata 5, 27100 Pavia, Italy*
[2] *Spectra-Physics Rankweil, Feldgut 9, Rankweil A-6830, Austria*
[*] *Corresponding author: federico.pirzio@unipv.it*

Compiled September 24, 2015

An Yb:CaF_2 laser pumped by two 400-mW single-mode laser diodes at 976 nm is reported to generate Fourier-limited 65-fs pulses, the shortest to date achieved with SESAM mode-locking and this laser material to date. With a multimode pump diode we have demonstrated higher average output powers of up to 1.4 W with 87-fs pulses. Key to these successful results was the implementation of practical design guidelines allowing safe mode-locking operation without Q-switching instabilities which appear to damage the SESAMs more easily in Yb:CaF_2 oscillators compared to other Yb-doped materials.

OCIS codes: *(140.3615) Lasers, ytterbium; (140.7090) Ultrafast lasers; (140.3580) Lasers, solid-state.*

http://dx.doi.org/10.1364/ao.XX.XXXXXX

1. INTRODUCTION

Broadband Yb-doped gain media are currently employed in many commercial ultrafast passively mode-locked oscillators operating at 1 μm. Significant improvement in the brightness of multiwatt pump laser diodes allows to overcome the limitation related to the quasi-three level nature of Yb^{3+} ion, by increasing gain per Watt (absorbed power) and reducing laser threshold. Semiconductor saturable absorber mirror (SESAM) technology is now very reliable and offers outstanding performance in mode-locking Yb lasers down to few tens of femtoseconds. With a market strongly pushing towards shorter pulse duration and higher average power, a crucial point of laser materials research is the identification of the best candidates offering both good thermo-mechanical properties and a wide, and possibly flat, emission bandwidth allowing sub-100-fs pulse generation. Outstanding results have been recently obtained with Yb:CALGO and Yb:CALYO, both in Kerr lens mode-locking (KLM) [1] and SESAM mode-locking [2, 3].

Fluoride crystals are also very attractive due to their optical and thermal properties, especially Yb:CaF_2. Its relatively high thermal conductivity (5 $Wm^{-1}K^{-1}$ for a 2.5% Yb doping concentration), along with a weakly negative thermo-optic coefficient, results in a significant reduction in thermal lensing. Furthermore, its very broad emission bandwidth, though not as flat as in Yb:CALGO and Yb:CALYO, was exploited to demonstrate pulses as short as 48 fs in KLM [4]. The material has a long fluorescence lifetime (τ_f = 2.4 ms) and a relatively low peak emission cross section ($\sigma_e = 0.17 \times 10^{-20}$ cm^2) [5].

The large τ_f value can be exploited for high-energy amplification of short pulses [6], reducing the complexity of the pump system for such applications. Although the product $\sigma_e\tau_f$ is still favorable for low threshold laser operation, the small value of σ_e yielding high energy storage capability can easily be responsible of SESAM optical damage in presence of Q-switched mode-locking (QML) instabilities [7]. This may explain why pulses as short as 99 fs were previously obtained with this material and SESAM-ML only by exploiting some additional KLM contribution [8], despite the small value of nonlinear refractive index of CaF_2 ($n_2 \sim 1.9 \times 10^{-20}$ m^2/W) that makes nonlinear amplitude modulation relatively weak in this case. Furthermore, KLM was more effectively implemented lately with special design adaptations such as ultra-high brightness single-mode fiber pumping [4].

In this work we present, to the best of our knowledge, the first sub-100-fs Yb:CaF_2 femtosecond oscillators mode-locked by SESAMs without assistance from Kerr lensing. We analyze carefully the stability condition against QML and discuss possible ways to optimize the resonator design in order to overcome optical damage issues of the SESAM. With these design guidelines we obtained 65-fs long pulses in a low power oscillator pumped by two polarization-combined, 400-mW single-mode fiber-coupled laser diodes. Furthermore, with a multi-mode fiber-coupled 12-W laser diode we were able to achieve up to 1.4 W average output power with 87 fs long pulses at 1050 nm.

2. EXPERIMENTS

We started with a low-power setup, pumping with a pair of single-mode fiber-coupled laser diodes, both emitting about

400 mW maximum power at 976 nm. Owing to the excellent beam quality, this pump system yields the highest gain per Watt of absorbed power compared to multi-mode diode pumping, and the lowest thermal stress in the crystal. This allows optimizing the oscillator for short pulses, with greater ease than multiwatt multi-mode pumping, requiring more careful thermal management of the crystal and proper thermal lensing considerations in the laser design.

By optimizing coiling the single-mode fiber pig-tails we were able to induce a strongly elliptical polarization in each laser diode, with a ratio of about 13:1 between the two axes. The two beams were then combined with a polarizer, spatially overlapped and focused into the active medium to a beam radius of 12 μm by means of a spherical lens. The crystal was a 3-mm long, 5%-doped Yb:CaF_2 sample with both facets anti-reflection (AR) coated for the pump and laser wavelengths, respectively. The X-folded resonator for the low power experiments is shown in Fig. 1. The curved mirrors M1 and M2 had a radius of curvature (ROC) of 50 mm and 100 mm, respectively.

In both continuous wave (CW) and ML operation, the resonator was designed to operate in the stability region corresponding to larger separation M1-M2. Therefore, we could fine-tune the cavity mode waist on the M3/SESAM mirror by properly adjusting its distance to M2 and the M1-M2 separation. This was particularly important for ML experiments, since the waist dimension fixes the intracavity pulse fluence on the SESAM, which is one of the critical design parameters for the stabilization of passive ML regime against QML instabilities [7].

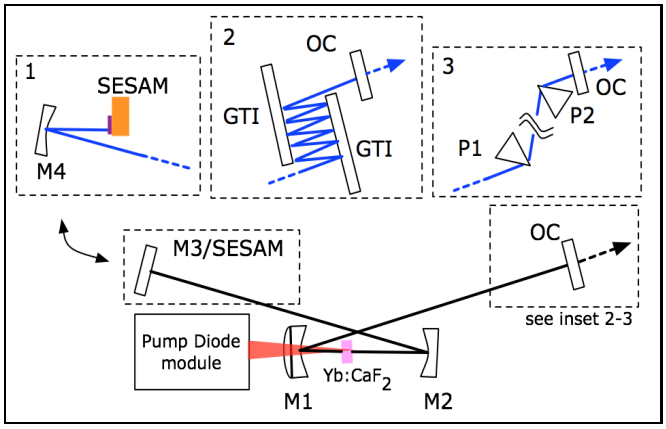

Fig. 1. Cavity setup. M1, M2: curved mirrors AR@976 nm, HR@1000-1100 nm; M3: Flat end mirror replaced by a SESAM for ML experiments in low-power setup; Inset 1: M4 spherical curved mirror HR@1000-1100 nm ROC = 300 mm used in ML experiments with multi-Watt pump power; Inset 2, 3: GTI: Gires-Tournois interferometric mirrors for GDD compensation in soliton ML regime; P1, P2: FS prisms pair for GDD compensation in soliton ML regime; OC: output coupler mirror 30′ wedge.

In CW regime, the cavity arm lengths were as follows: M2-M3 = 200 mm; M1-M2 = 91 mm; M1-OC = 750 mm. Through ABCD modeling of the resonator we could estimate a fundamental cavity mode radius in the active medium ranging from 11 to 13 μm within the stability region, well matched to the pump mode radius. The results obtained in CW regime for a set of different output couplers (OCs) with transmission T are shown in Fig. 2.

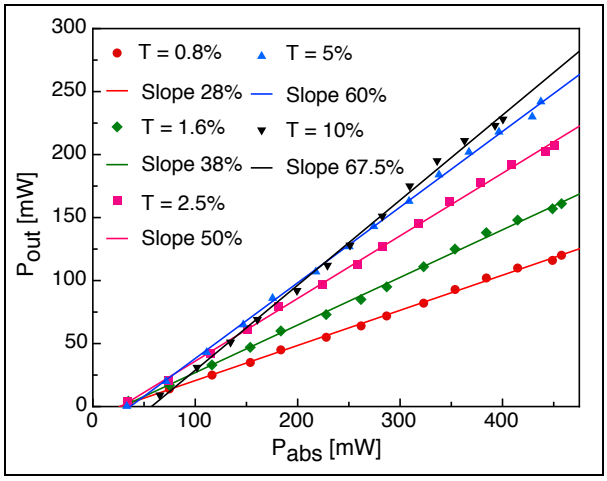

Fig. 2. CW performance with different OCs.

With the optimum T = 5% we obtained up to 240 mW with an absorbed pump power of 435 mW (55% internal optical-to-optical efficiency). A maximum slope efficiency of 67.5% was obtained with T = 10%. In order to determine the total losses δ (cavity + crystal) and the intrinsic slope efficiency η_0, we performed the Caird analysis [9], redand fit the measured slope efficiency η as a function of the laser OC reflectivity with the following equation:

$$\eta = \frac{\lambda_p}{\lambda_l}\eta_0\frac{-\ln(R_{OC})}{\delta - \ln(R_{OC})} \quad (1)$$

redwhere λ_p and λ_l are the pump and laser output wavelength respectively. It is worth noting that in our experiments the output laser wavelength in cw regime was only slightly dependent on the OC reflectivity, varying between 1053 and 1045 nm for the OC transmission varying from 0.8% to 10%. Thus the ratio λ_p/λ_l in Eq. (1) can be reasonably considered constant. Moreover, please note that δ does not include reabsorption losses, which contribute to determine the laser threshold but are not affecting the laser performance above threshold. The results are shown in Fig. 3. The best fit yields a high, nearly quantum-limited intrinsic slope efficiency (accounting for mode-matching efficiency and quantum efficiency) of $\eta_0 = 0.83$ and total resonator losses, excluding the reabsorption losses in the Yb-doped crystal, of $\delta = 1.5\%$ (mostly due to AR losses from the crystal facets).

For ML experiments we replaced the M3 mirror with a SESAM having 3% modulation loss and a saturation fluence of ~140 μJ/cm^2 (a set of such SESAMs with similar parameters was available). In order to polarize the laser output we inserted a 2-mm thick fused silica plate at Brewster angle close to the output coupler. For intracavity group delay dispersion (GDD) compensation, a pair of GTI mirrors providing -55 fs^2 negative dispersion per bounce were chosen. Stable and self-starting soliton ML regime was obtained with a minimum number of 5 bounces per mirror, corresponding to a total negative dispersion per roundtrip of about -1100 fs^2. Pulses as short as 65 fs with an optical spectrum of 20 nm (FWHM) centered at 1050 nm (Fig. 4) were obtained with T = 0.8% at an average output power of 35 mW. The corresponding time-bandwidth product was 0.35, close to the Fourier-transform limit for *sech*^{2}

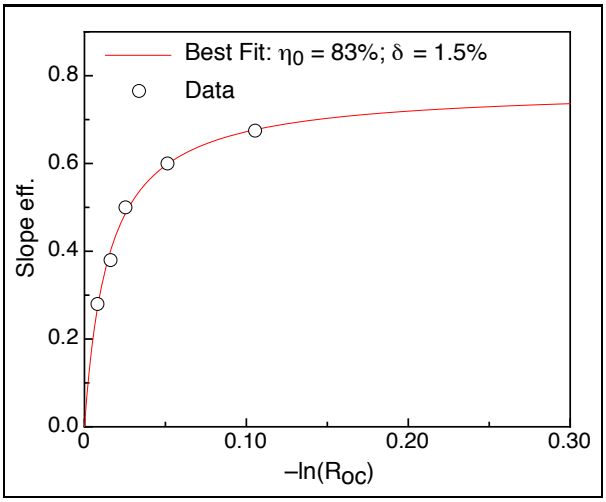

Fig. 3. Slope efficiency as function of output coupler mirror reflectivity.

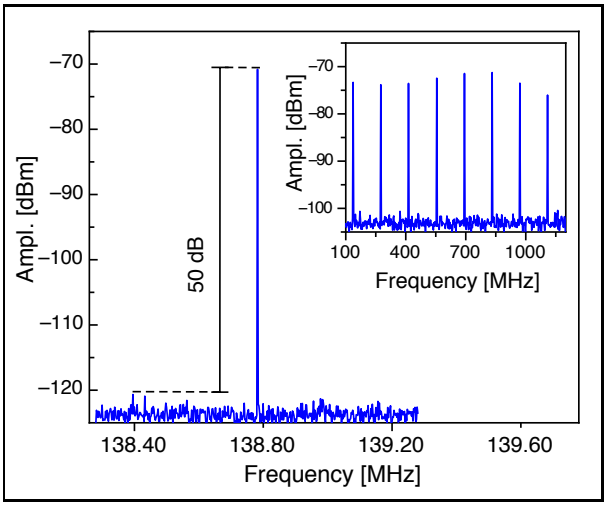

Fig. 5. RF spectrum of the CW mode-locked pulse train at the fundamental beat note and (inset) with 1 GHz span.

shaped pulses. No variations in beam profile were observed when switching between CW and ML, for example during adjustment of the dispersion. This makes contributions from KLM unlike in our setup.

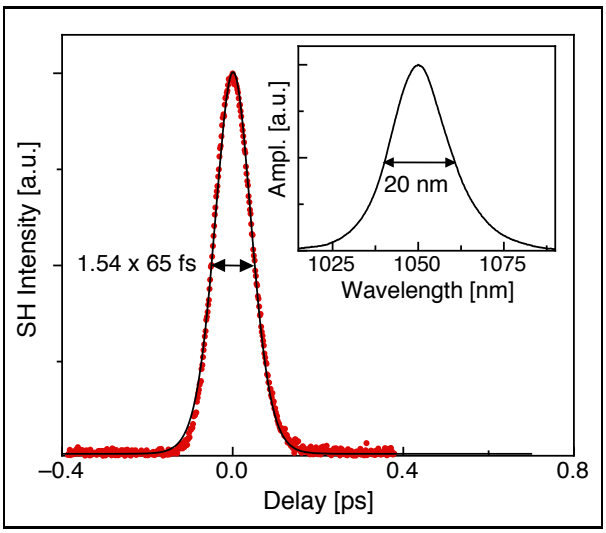

Fig. 4. Autocorrelation trace and optical spectrum (inset) of the shortest pulses obtained with T = 0.8%.

In order to assess the stability of the mode-locked operation, we measured radio frequency (RF) spectra at different span ranges using a 3 GHz bandwidth spectrum analyzer (Agilent N9320B). In Fig. 5 we show the fundamental beat note at $\sim$ 139 MHz, with a high extinction ratio of $\sim$ 50 dB, indicating the absence QML instabilities. The RF spectrum in a 1 GHz span with 10 kHz resolution bandwidth shown in the inset of Fig. 5 is also indicative of clean single pulse operation of the laser.

Wavelength-tuning experiments were performed by including a single prism for both GDD compensation and easy tuning of the soliton pulse, as for example in Refs. [3, 10]. The oscillator was only slightly tunable in a narrow range of $<$ 10 nm around 1050 nm, despite the broad fluorescence spectrum.

Mode size on the SESAM (in our setup about 40 μm radius), pump power and, to a lesser extent, cavity length proved to be critical for stable CW-ML and damage-free operation of the SESAM. Indeed, an initial attempt to set up the oscillator with a single pump diode failed to achieve ML, and the SESAM was often suffering damage. The following Section 3 provides quantitative insights into critical aspects of the resonator design specific to Yb:CaF_2. As a further step confirming the validity of our design guidelines, and to investigate the potential power scaling of the laser, we designed and built a second resonator pumped by a 12-W, 100-μm fiber-coupled single-emitter pump laser diode at 976 nm. The pump beam was imaged in the active medium by means of an achromatic lens telescope with a magnification factor of 1.2. With respect to the low pump power experiments (see Fig. 1) we replaced the pump mirror M1 (ROC = 50 mm) with a mirror having ROC = 300 mm and mirror M2 with one having ROC = 250 mm. With respect to the low power experiments, we operated the resonator in the other stability region, hence the cavity mode was focused on the SESAM by means of the curved mirror M4 (ROC = 300 mm).

For intracavity GDD compensation we employed a pair of fused silica prisms separated by a distance of about 500 mm, yielding a maximum negative GDD of about -1100 fs^2. In this resonator configuration ABCD modeling yielded a cavity mode waist radius in the active medium and on the SESAM of about 60 and 80 μm, respectively. Stable and self-starting ML pulse trains at 80 MHz repetition rate were obtained with a maximum output power of 1.4 W at an incident pump power of 11 W with T = 5%. The autocorrelation trace and optical spectrum of the almost Fourier-transform limited pulses (time-bandwidth product 0.33) are shown in Fig. 6.

3. STABILITY AGAINST QML

As reported in Ref. [7], the interplay between gain filtering and soliton dynamics at the onset of QML can lead to a substantial decrease of the critical intracavity pulse energy E_p required for stabilization of CW-ML, with respect to the case of picosecond lasers:

$$E_G g K^2 E_p^3 + E_p^2 > E_G E_S \Delta R \qquad (2)$$

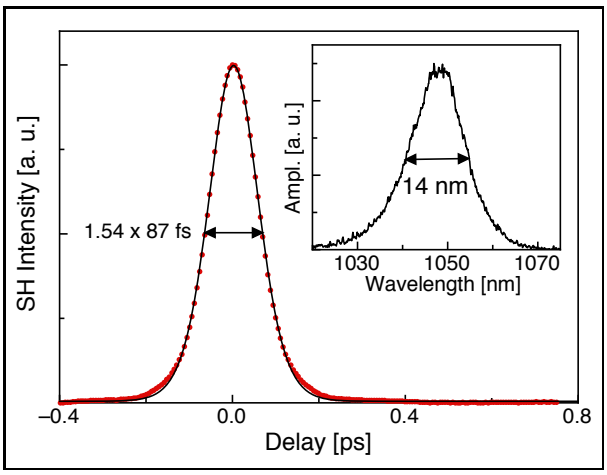

Fig. 6. Autocorrelation trace and optical spectrum (inset) of the shortest pulses obtained with T = 5%.

where $E_G = F_G A_G$ is the saturation energy of the amplifier (F_G being the saturation fluence and A_G the mode area in the gain medium). Similarly, $E_S = F_S A_S$ is the saturation energy of the SESAM, ΔR its modulation depth, g the saturated gain and

$$K = \frac{4\pi n_2 L_K}{D_2 A_G \lambda \Delta\nu_G} \frac{0.315}{1.76} \tag{3}$$

where n_2 is the Kerr coefficient, L_K the length of Kerr medium (gain material in this case), D_2 the net (negative) GDD, $\Delta\nu_G$ the available gain bandwidth (considering reabsorption losses) and λ the central wavelength of the pulse spectrum. By using the soliton equation

$$\tau_p = 1.76 \frac{D_2 \lambda A_G}{4\pi n_2 L_K E_p} \tag{4}$$

and introducing a parameter expressing the fractional bandwidth used by the pulse, $\xi = \Delta\nu/\Delta\nu_G$, we can conveniently rewrite Eq. (2) and solve it to yield an explicit value of the critical pulse energy:

$$E_p > -\frac{g\xi^2 E_G}{2} + \sqrt{\left(\frac{g\xi^2 E_G}{2}\right)^2 + E_G E_S \Delta R} \tag{5}$$

It is worth noticing that for $\xi \to 0$ Eq. (5) reduces to the simpler case of picosecond lasers.

In general, for femtosecond soliton lasers ξ corresponds to a significant fraction of the gain bandwidth as soon as a sufficiently large amount of negative dispersion is provided to stabilize ML in the early alignment step. Afterwards, the negative GDD is gradually reduced in order to shorten the pulse before splitting occurs, and typical values $0.3 < \xi < 0.8$ are eventually achieved. In order to evaluate the actual value of ξ, one should first calculate the effective gain spectrum from spectroscopic data

$$g_{eff}(\lambda) = 2L_g N_{tot}\{\beta[\sigma_e(\lambda) + \sigma_a(\lambda)] - \sigma_a(\lambda)\} \tag{6}$$

where L_g is the active medium length, N_{tot} is the dopant ion density, $\sigma_e(\lambda)$ and $\sigma_a(\lambda)$ are the active medium wavelength-dependent emission and absorption cross sections and $\beta = N_2/N_{tot}$ is the fraction of dopant ions that occupy the higher laser level at the steady state and depends on the OC transmittivity and cavity losses. The actual value of β at which the laser operates can be evaluated by the constrain that gain in Eq. (6) must equal the losses at the laser threshold. In Fig. 7 we present a comparison between effective gain spectra of Yb:CaF_2 calculated in our experimental conditions and the actual measured ML pulse spectra obtained in the low power (Fig. 4) and high power (Fig. 6) experiments. The experimental value of ξ was about 0.66 in low power and 0.35 in high power experiments, once the laser was optimized for minimum pulse duration. For Yb-doped laser materials and oscillators

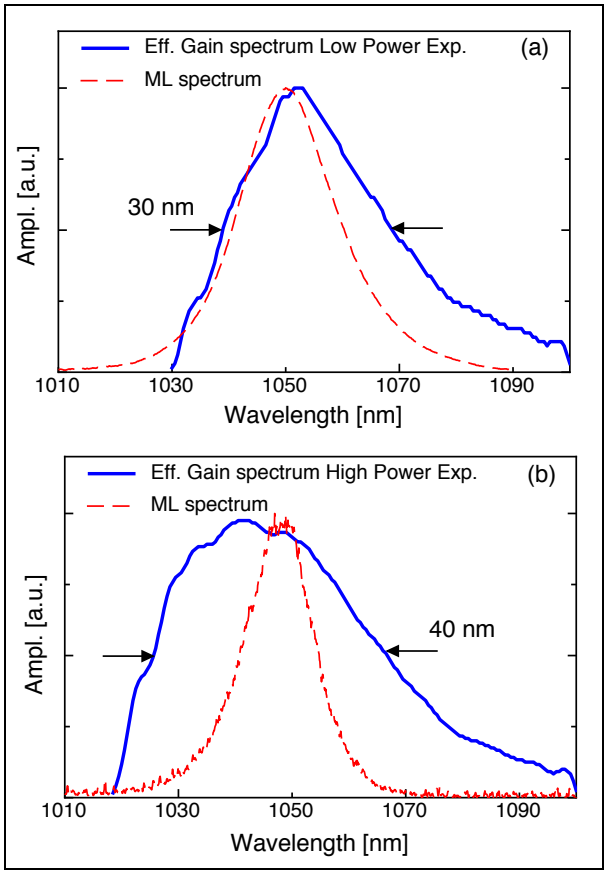

Fig. 7. Effective gain spectrum calculated in our experimental conditions for the low (a) and high (b) power experiments. For comparison the corresponding measured ML spectra are also shown in red.

based on the layout shown in Fig. 1, where the mode area ratio A_G/A_S can vary within the range 0.1-10 typically, and for typical $F_S \sim 10 - 100\mu J/cm^2$ of SESAMs we find that the square root of Eq. (5) is dominated by the first term inside, hence the following approximation holds:

$$E_p > \frac{E_S \Delta R}{g\xi^2} \tag{7}$$

This also implies that the SESAM is operated with sufficient saturation of the nonlinear absorption.

However, when pulse wavelength corresponds to the tails of the gain spectrum, where the approximation implicit in Eq. (7) might fail, complete expression of Eq. (5) must be used instead. This simple result helps to explain the difficulties inherent in the design of SESAM-ML oscillators based on Yb materials with particularly small emission cross section, such as

Yb:CaF_2. Notice that the stability condition expressed by Eq. (7) does not involve the saturation energy E_G of the amplifier. However, if a QML instability occurs for instance during alignment of the SESAM, the energy carried by the Q-switching envelope is $\sim E_G$ and can potentially damage the SESAM more easily than in Yb-lasers with larger emission cross section. The most straightforward action to prevent SESAM damage is to increase A_S, but this increases E_S as well as the threshold E_p, hence higher pump power is required. Indeed, before modifying the oscillator design, in low power experiments we started to observe stable CW-ML when we turned the second pump diode on.

Operation stability can be further improved by increasing the resonator length: the intracavity pulse energy increase allows the threshold condition of Eq. (7) to be achieved more easily. Furthermore, in this case the mode area A_G decreases, hence reducing the envelope energy of possible QML instabilities which may arise during alignment, or after ML is stopped. The critical energy threshold (7) can be conveniently lowered by chosing a SESAM with smaller modulation depth (which was not available for our experiments), although this would limit the pulse shortening effect. (In our experience with Yb lasers, the higher the modulation depth which can reasonably sustain stable CW-ML, the shorter the pulse). However, too small modulation depth can prevent ML build-up [11], hence a trade off must be considered. Pumping with high-brightness single-mode lasers as we did in the low-power setup is also beneficial by reducing the area A_G to a minimum.

Using the parameters of our experiments, it turns out that the intracavity pulse energy E_p exceeds the stability limit by a factor ~ 3.2 and ~ 2.7 for the low- and high-power setup, respectively. Notice that we started always with larger ratio A_S/A_G, allowing threshold (7) to be exceeded by even larger amount. Afterwards, the mode size on the SESAM was gradually reduced by decreasing the separation SESAM-M2, in order to achieve the shortest pulse possible. This optimization process was stopped before reaching the critical mirror separation where damage started to occur.

Eventually, also the narrow tuning range can be explained by these arguments: detuning the central wavelength from the peak gain can further decrease the emission cross section and increase susceptibility to QML, since the stability condition is exceeded only by a small amount, compared to other situations we investigated previously [3, 10]. We remark that this soliton stability analysis was developed for homogenously broadened materials, but it was noticed in Ref. [7] that these general concepts and predictions can still be applied to disordered materials such as Yb:CaF_2, with further reduction of critical energy owing to the presence of ions with cross sections larger than the effective average spectroscopic cross section.

4. CONCLUSIONS

We have reported, to the best of our knowledge, the first sub-100-fs SESAM mode-locked diode-pumped Yb:CaF_2 laser. Taking advantage of single-mode laser diode pumping we demonstrated 65-fs long pulses in a low power resonator. With a power-scaled resonator pumped by a multi-mode fiber-coupled single-emitter diode, we were able to demonstrate up to 1.4 W average output power with stable and self-starting 87-fs ML pulse trains.

It was shown that stability against QML is a major concern for ultrafast lasers employing Yb-doped materials with very small emission cross section. An explicit simple expression of the critical intracavity energy was derived as the approximation of a more general result. Along with optical damage considerations, we have proposed design guidelines for this particular class of ultrafast oscillators.

The femtosecond Yb:CaF_2 laser sources presented in this work are suitable for amplification to multi-Watt average output power in multipass or regenerative amplifiers. However, we should remark that, based on our experience, materials such as Yb:CALGO and Yb:CALYO appear to largely outperform Yb:CaF_2 for stable, reliable, extremely short pulse generation (near and sub-40-fs) and broad tunability (~ 40 nm) encompassing most of the effective gain bandwidth above laser threshold.

REFERENCES

1. P. Sévillano, P. Georges, F. Druon, D. Descamps, and E. Cormier, Opt. Lett. **20**, 6001–6004 (2014).
2. A. Agnesi, A. Greborio, F. Pirzio, G. Reali, J. Aus der Au, and A. Guandalini, Opt. Express **20**, 10077–10082 (2012).
3. F. Pirzio, S. D. Di Dio Cafiso, M. Kemnitzer, A. Guandalini, F. Kienle, S. Veronesi, M. Tonelli, J. Aus der Au, and A. Agnesi, Opt. Express **23**, 9790–9795 (2015).
4. P. Sévillano, G. Machinet, R. Dubrasquet, P. Camy, J.-L. Doualan, R. Moncorgé, P. Georges, F. Druon, D. Descamps, and E. Cormier, in Advanced Solid-State Lasers Congress Technical Digest (OSA 2013) AF3A.6.
5. F. Druon, S. Ricaud, D. N. Papadopoulos, A. Pellegrina, P. Camy, J. L. Doualan, R. Moncorgé, A. Courjaud, E. Mottay, and P. Georges, Opt. Mater. Express **1**, 489–502 (2011).
6. A. Kessler, M. Hornung, S. Keppler, F. Schorcht, M. Hellwing, H. Liebetrau, J. Körner, A. Sävert, M. Siebold, M. Schnepp, J. Hein, and M. C. Kaluza, Opt. Lett. **39**, 1333–1336 (2014).
7. C. Hönninger, R. Paschotta, F. Morier-Genoud, M. Moser, and U. Keller, J. Opt. Soc. Am. B **16**, 45–56 (1999).
8. F. Friebel, F. Druon, J. Boudeile, D. N. Papadopoulos, M. Hanna, P. Georges, P. Camy, J. L. Doualan, A. Benayad, R. Moncorgé, C. Cassagne, and G. Boudebs, Opt. Lett. **34**, 1474–1476 (2009).
9. J. A. Caird, S. A. Payne, P. R. Staber, A. J. Ramponi, L. L. Chase, and W. F. Krupke, IEEE J. Quantum Electron. **24**, 1077–1099 (1988).
10. A. Agnesi, A. Greborio, F. Pirzio, E. Ugolotti, G. Reali, A. Guandalini, and J. Aus der Au, J. Opt. Soc. Am. B **30**, 1513–1516 (2013).
11. A. Agnesi, L. Carrà, F. Pirzio, G. Reali, A. Toncelli, M. Tonelli, S.Y. Choi, F. Rotermund, U. Griebner, and V. Petrov, J. Opt. Soc. Am. B **27**, 2739–2742 (2010).